On the Phase Noise Performance of Transformer-Based CMOS Differential-Pair Harmonic Oscillators

Andrea Mazzanti, *Senior Member, IEEE,* and Andrea Bevilacqua, *Senior Member, IEEE*

***Abstract*—The white noise to phase noise conversion of one- and two-port CMOS differential-pair harmonic oscillators with transformer-based resonators is addressed in this paper. First, the operation of double-tuned transformer resonators is reviewed and design guidelines are proposed to maximize the quality factor. A rigorous approach is then employed to approximate the transformer network with a second order RLC model near the resonances, greatly simplifying the problem of handling the complex equations of a higher order resonator. The results are applied to phase noise calculations, leading to simple, yet accurate, closed-form $1/f^2$ phase noise expressions in excellent agreement with the simulation results. It is formally proved, in a general case, that high-order resonators do not provide any fundamental advantage in comparison with simple LC-tanks. The two-port transformer based oscillator may be exploited to limit the phase noise contribution of the core transistors through optimization of the bias point and by leveraging the transformer voltage gain.**

I. Introduction

Oscillators are fundamental components for any communication system and steadily attract a wide research interest to improve their performance. A variety of new harmonic oscillators has been proposed in the last decade. Among them, circuits based on higher order resonators realized with double-tuned transformers have been investigated to address wide tuning range, or low phase noise. While the advantage in terms of frequency tuning is evident, being them able to operate over wide bands [1]–[6], the benefit for spectral purity is not clear and still debated. An improvement in the phase noise has been claimed, in comparison with oscillators based on a single inductor resonator, due to the higher quality factor related to the additional magnetic energy stored in the mutual inductance between the transformer coils [7]–[10]. On the other hand, it has been shown that an inductor occupying the same silicon area of the transformer (straightforwardly achieved, for example, by connecting in series the two windings of the transformer itself) may display the same quality factor [11], [12]. The resonator quality factor is a key parameter determining oscillator frequency stability, but, to precisely estimate the phase noise, additional features, such as circuit topology, resonator impedance and power dissipation, have to be considered.

Manuscript received;

Andrea Mazzanti is with the Department of Industrial and Information Engineering, University of Pavia, 27100 Pavia, Italy.

Andrea Bevilacqua is with the Department of Information Engineering, University of Padova, 35131 Padova, Italy (e-mail: andrea.bevilacqua@dei.unipd.it).

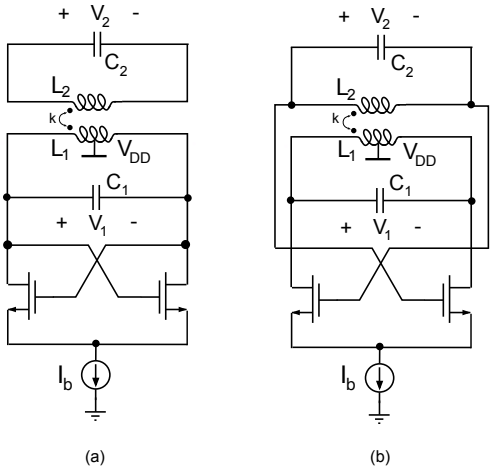

Fig. 1. Schematic of oscillators with transformer-based resonators: (a) one-port oscillator, (b) two-port oscillator.

The phase noise of LC-tank oscillators has been extensively studied and accurate equations are now available for most topologies [13]–[17]. On the contrary, the performance of the transformer-based oscillators has not been investigated as much. The task is made challenging by the complex equations describing the high order resonator. In [5], [9], [10], the problem is addressed by approximating the resonator as a second order LC-tank in a narrow band around the resonance frequency. However, it is erroneously assumed, as proved in this paper, that the equivalent LC-tank features the same capacitance as the one in parallel with either the primary or secondary winding of the two transformer (C_1, C_2 in Fig. 1). As a consequence, the equivalent circuits do not capture the resistance at resonance and the quality factor of the transformer resonator simultaneously.

This paper reviews the operation of the transformer-based resonator and proposes accurate, yet simple expressions, rigorously derived, for the components of an equivalent second-order circuit that approximates very well the transformer network near the resonances. The results are applied to phase noise formulation in the $1/f^2$ region for the two oscillators in Fig. 1, where the transformer is used as a one-port, or a two-port resonator, respectively. The performance of these oscillators is then discussed and compared against the well-known LC-tank topology. It is formally concluded that, as far as the $1/f^2$ phase noise or oscillator Figure-of-Merit

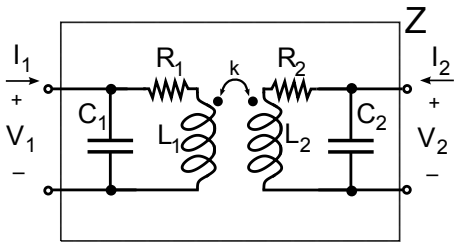

Fig. 2. Schematic of the transformer-based resonator.

are considered, there is not any intrinsic benefit from the multi-resonance nature of higher-order networks. The one-port transformer-based oscillator does not provide advantages in comparison with the simple LC-tank topology while the two-port configuration may be exploited to limit the phase noise contribution of the core transistors only by leveraging the transformer voltage gain in combination with optimal biasing.

The paper is organized as follows. The analysis of the transformer-based resonator is reported in Section II. Section III describes the simplified circuit proposed to ease phase noise calculations, as well as the computation of phase noise for the one-port and two-port oscillator topologies. In Section IV, transistor-level simulations are carried out to validate the proposed theory. Finally, a discussion is carried out in Section V, which wraps up the paper.

II. Analysis of the Transformer-Based Resonator

The transformer-based resonator is shown in Fig. 2. First, the most relevant parameters of the resonator are analytically derived. Then, guidelines for the optimum design, i.e. quality factor maximization, are hereto provided. In Section III-A, a rigorous procedure to approximate the network in a narrow band around the resonance frequencies with the equivalent circuit in Fig. 6 to the aim of studying phase noise is described.

A. Oscillation Modes and Resonator Parameters

The resonator displays two possible modes of oscillation with angular frequencies given by [1]:

$$\begin{aligned}\omega_{L,H}^2 &= \frac{1+\xi \pm \sqrt{(1+\xi)^2-4\xi(1-k^2)}}{2(1-k^2)}\omega_2^2 \\ &= \Omega_{L,H}^2(\xi,k)\cdot\omega_2^2\end{aligned} \tag{1}$$

where $\omega_1^2 = (L_1C_1)^{-1}$, $\omega_2^2 = (L_2C_2)^{-1}$, $\xi = (\omega_1/\omega_2)^2$, k is the magnetic coupling between L_1 and L_2, and $\Omega_{L,H} = \omega_{L,H}/\omega_2$.

When the resonator is embedded in the two oscillators in Fig. 1, the impedance at port 1, $Z_1 = (G_1 + jB_1)^{-1}$, and the transimpedance $Z_{21} = (G_{21} + jB_{21})^{-1}$ are of interest. Notice that the capacitive parasitics of the active devices are assumed to be taken into account by embedding them in C_1 and C_2 in Fig. 2. Assuming all the resonator losses come from the magnetic components, and a moderately high quality factor for the two transformer inductors, i.e. $Q_1 = \omega L_1/R_1 \gg 1$, $Q_2 = \omega L_2/R_2 \gg 1$, the analysis of the circuit in Fig. 2 yields:

$$G_1 \approx \frac{1}{R_1Q_1^2}\cdot\frac{\Omega^4\left(1+\frac{Q_1}{Q_2}k^2\right)-2\,\Omega^2+1}{\left[\Omega^2(1-k^2)-1\right]^2}, \tag{2}$$

$$B_1 \approx \frac{1}{\omega L_1}\cdot\frac{\left(\frac{\Omega^2}{\Omega_L^2}-1\right)\left(\frac{\Omega^2}{\Omega_H^2}-1\right)}{\Omega^2(1-k^2)-1}, \tag{3}$$

$$G_{21} \approx \frac{1}{R_1Q_1^2}\cdot\frac{-\Omega^4\left(1+\frac{Q_1}{Q_2}\right)+\Omega^2\left(1+\frac{Q_1}{Q_2}\xi\right)}{\xi k\cdot n}, \tag{4}$$

and

$$B_{21} \approx -\frac{1}{\omega L_1}\cdot\frac{\Omega^4(1-k^2)-\Omega^2(1+\xi)+\xi}{\xi k\cdot n}, \tag{5}$$

where $\Omega = \omega/\omega_2$ and $n = \sqrt{L_2/L_1}$.

As discussed in [1], in the one-port oscillator of Fig. 1(a), when port 1 is terminated on a negative resistance (e.g. a cross-coupled differential pair), oscillations will build up in the lower frequency mode or in the higher frequency mode, i.e. at ω_L or at ω_H, depending on the value of $\rho = G_1(\omega_L)/G_1(\omega_H)$. If $\rho < 1$, the oscillator will work at ω_L, otherwise it will work at ω_H. As such, there is a set of values of the parameters (ξ, k) for which oscillations occur at ω_L, and a set of (ξ, k) for which oscillations occur at ω_H. When, instead, port 2 is terminated on a negative resistance, the behavior is symmetrical, with $\rho > 1$ yielding oscillations at ω_L, and oscillations starting up at ω_H otherwise. Conversely, in the case of the two-port oscillator of Fig. 1(b), the mode of operation is selected by the connection of the active feedback network around the resonator, as in this case the phase shift introduced by the resonator in the feedback loop is 0° at ω_L, and 180° at ω_H.

B. Design for Maximum Quality Factor

The resonator quality factor is computed as [1], [18]:

$$Q = \frac{\omega}{2}\left|\frac{d}{d\omega}\ln\left(\frac{1}{Z_1}\right)\right|_{\omega=\omega_{L,H}} \approx \frac{\omega}{2}\left|\frac{\frac{dB_1}{d\omega}}{G_1}\right|_{\omega=\omega_{L,H}} \tag{6}$$

leading to[1]:

$$\begin{aligned}Q &\approx Q_1\frac{\left[2\Omega_{L,H}^4(1-k^2)-\Omega_{L,H}^2(1+\xi)\right]\left[\Omega_{L,H}^2(1-k^2)-1\right]}{\xi\left[\Omega_{L,H}^4\left(1+\frac{Q_1}{Q_2}k^2\right)-2\,\Omega_{L.H}^2+1\right]} \\ &= Q_1\cdot\Psi(\xi,k,Q_1/Q_2)\end{aligned} \tag{7}$$

Equation (7) gives the network Q at the two resonance frequencies as a function of primary and secondary quality factors, coupling between coils and the design parameter ξ. For any value of Q_1/Q_2, $\Psi(\xi, k, Q_1/Q_2)$ in (7) captures the dependence of Q on ξ and k only. The higher is

[1]The quality factor can be similarly calculated starting from Z_{21}, obtaining an equivalent result [1]. Moreover, note that (6) can be recast as $Q = \frac{\omega}{2}\left|\frac{d}{d\omega}\left|\frac{1}{Z_1}\right| + j\frac{d}{d\omega}\angle\frac{1}{Z_1}\right|_{\omega=\omega_{L,H}} = \frac{\omega}{2}\left|\frac{d}{d\omega}\angle\frac{1}{Z_1}\right|_{\omega=\omega_{L,H}}$.

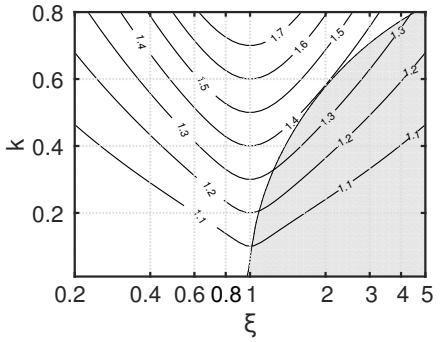

(a)

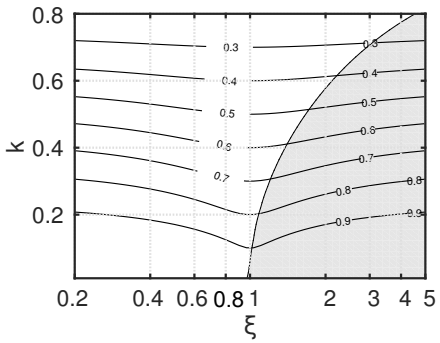

(b)

Fig. 3. Plot of $\Psi(\xi, k, Q_1/Q_2)$ for $Q_1 = Q_2$ evaluated at: (a) ω_L, (b) ω_H. The shaded area is where the oscillation starts at ω_H, in the case of a one-port oscillator topology.

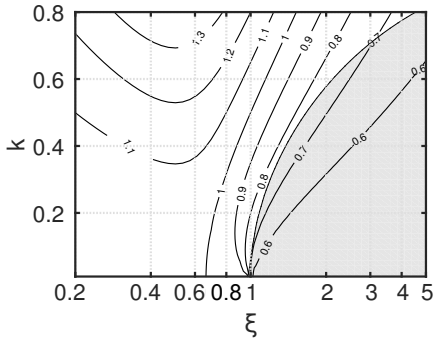

(a)

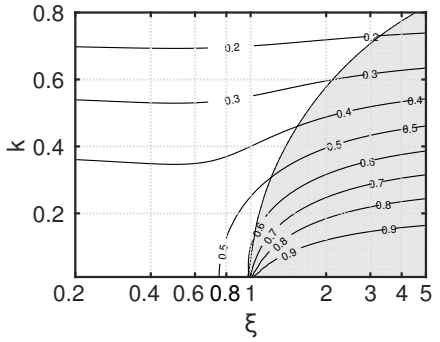

(b)

Fig. 4. Plot of $\Psi(\xi, k, Q_1/Q_2)$ for $Q_1/Q_2 = 2$ evaluated at: (a) ω_L, (b) ω_H. The shaded area is where the oscillation starts at ω_H, in the case of a one-port oscillator topology.

$\Psi(\xi, k, Q_1/Q_2)$ and the higher is the quality factor of the double-tuned transformer resonator. Q_1 and Q_2 are set by the technology and shape of the coils and are maximized by optimizing the inductors geometry. If the two windings of the transformer share the same trace width and the same metal layers, it is reasonable to assume $Q_1 \approx Q_2$. For any technology, in practice there is a maximum attainable value for Q_1 and Q_2. As detailed in the Appendix, (7) is an increasing monotonic function of Q_1 and Q_2, such that Q is maximized when $Q_1 = Q_2$, and they are both equal to their maximum possible value.

A plot of $\Psi(\xi, k, Q_1/Q_2)$ is shown in Fig. 3 for $Q_1 = Q_2$. In the case of the one-port oscillator, the shaded area is where the oscillation builts up at the higher resonance frequency, ω_H. In the case of the two-port oscillator, the two-port configuration allows to select either of the two oscillation modes, regardless of the values of (ξ, k), as discussed in Section II-A.

Figure 3 shows that, for a given operation frequency it is preferable to leverage the lower frequency mode to maximize the resonator Q. In the lower frequency mode, the magnetic fluxes generated by L_1 and L_2 couple constructively increasing the stored magnetic energy, and leading to $Q(\omega_L) > Q_1(\omega_L), Q_2(\omega_L)$. The opposite happens at ω_H. Moreover, for any given value of the magnetic coupling, k, Fig. 3 shows that $\xi = 1$ is the design condition maximizing Q.

It is worth noticing that, although $Q_1 \approx Q_2$ is a typical case, in general the value of ξ maximizing the resonator Q depends on the ratio Q_1/Q_2. In a scenario where the operation frequency is fixed, but any of the two oscillation modes can be employed to obtain the operation frequency (by properly adjusting the resonator parameters), for $Q_1 > Q_2$, and any given value of k, the maximum Q is obtained for $\xi < 1$ leveraging the lower frequency mode, as shown in Fig. 4, where $\Psi(\xi, k, Q_1/Q_2)$ is depicted for $Q_1/Q_2 = 2$. For $Q_1 < Q_2$, instead, the maximum Q is still obtained using the lower frequency mode, but for $\xi > 1$: Fig. 5 illustrates $\Psi(\xi, k, Q_1/Q_2)$ in the particular case of $Q_1/Q_2 = 1/2$. In other words, the optimization of the resonator Q is achieved by pushing at higher frequency the resonance ω_1 or ω_2 of the coil showing the lowest quality factor.

Finally, to put the foregoing discussion in perspective, we consider some numerical examples. First, assume $k = 0.5$ and a maximum attainable value of 10 for Q_1 and Q_2. The optimal scenario is obviously $Q_1 = Q_2 = 10$ with the design choice $\xi = 1$, which yields (see Fig. 3(a)) $\Psi = 1.5$ and thus $Q = 15$. Now let us suppose that $Q_1 = Q_2 = 10$ is not feasible for practical reasons (e.g. layout constraints) and the designer can only choose between the following options: $Q_1 = Q_2 = 7$ or $Q_1 = 10$, $Q_2 = 5$. In the first case, with optimal choice of $\xi = 1$, from Fig. 3(a) one gets $\Psi = 1.05$ and thus $Q = 10.5$. In the latter case, keeping $\xi = 1$ yields (see Fig. 4(a)) $\Psi = 1$ and thus $Q = 10$, while using the optimal value of ξ, namely $\xi = 0.5$ as shown in Fig. 4(a), gives a 20% improvement: $\Psi = 1.2$, hence $Q = 12$.

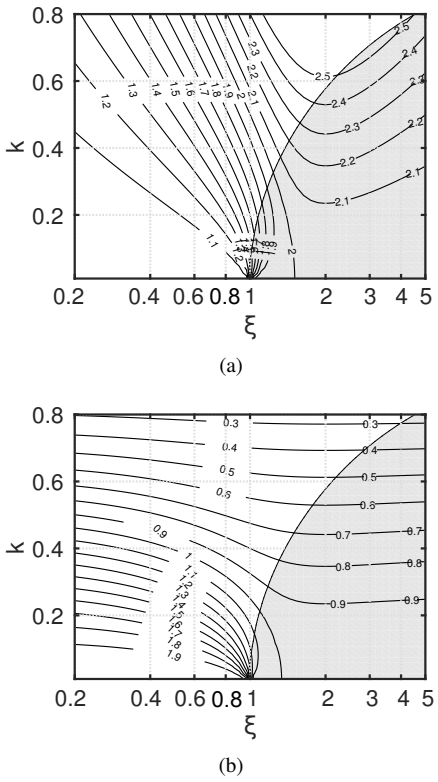

Fig. 5. Plot of $\Psi(\xi, k, Q_1/Q_2)$ for $Q_1/Q_2 = 1/2$ evaluated at: (a) ω_L, (b) ω_H. The shaded area is where the oscillation starts at ω_H, in the case of a one-port oscillator topology.

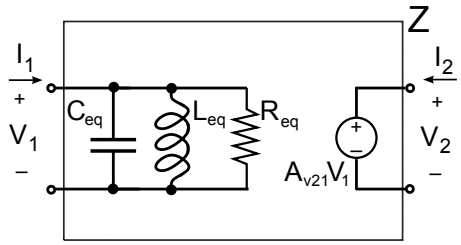

Fig. 6. Schematic of the simplified circuit modeling the transformer-based resonator.

III. Simplified Circuit for Phase Noise Analysis

The goal of the following discussion is to approximate the behavior of the transformer-based resonator, in the neighborhood of the parallel resonances $\omega_{L,H}$, with an equivalent second order LC-tank of elements $R_{\rm eq}$, $C_{\rm eq}$, and $L_{\rm eq}$, as illustrated in Fig. 6. The aim of this effort is to simplify the analysis of the operation and phase noise performance of the oscillators in Fig. 1. As a consequence, the model we will derive is not strictly equivalent to the network in Fig. 2. For example, reciprocity of the network is not preserved. Rather, the simplified circuit accurately captures just the relevant parameters for the oscillator analysis, namely the admittance of port 1, and the voltage transfer from port 1 to port 2.

A. Derivation of the Simplified Circuit

At resonance, the admittance of port 1 is purely resistive. Therefore, we have: $R_{\rm eq,L,H} = 1/G_1(\omega_{L,H})$, where G_1 is given by (2). To derive $C_{\rm eq}$ and $L_{\rm eq}$, the idea is to approximate (3) in the neighborhood of $\omega_{L,H}$ with a second order susceptance, so that it that can be interpreted as the parallel combination of an inductance and a capacitance. To this aim, in the lower resonance frequency case, we set $\Omega = \Omega_L$ in the factors of (3) accounting for the parallel resonance at ω_H and the series resonance at $\omega_2/\sqrt{1-k^2}$:

$$B_1 \approx \frac{1}{\omega L_1} \cdot \frac{\left(\frac{\Omega^2}{\Omega_L^2} - 1\right)\left(\frac{\Omega_L^2}{\Omega_H^2} - 1\right)}{\Omega_L^2(1-k^2) - 1} = \frac{1}{\omega L_1 \alpha_L}\left(\frac{\omega^2}{\omega_L^2} - 1\right) \tag{8}$$

where

$$\alpha_L = \alpha_L(\xi, k) = \frac{\Omega_L^2(1-k^2) - 1}{\Omega_L^4 \dfrac{1-k^2}{\xi} - 1} \tag{9}$$

From (8) it follows immediately[2]:

$$L_{\rm eq,L} = \alpha_L L_1 \qquad C_{\rm eq,L} = \frac{1}{\omega_L^2 \alpha_L L_1} \tag{10}$$

Similarly, in the neighborhood of ω_H, we obtain:

$$L_{\rm eq,H} = \alpha_H L_1 \qquad C_{\rm eq,H} = \frac{1}{\omega_H^2 \alpha_H L_1} \tag{11}$$

with

$$\alpha_H = \alpha_H(\xi, k) = \frac{\Omega_H^2(1-k^2) - 1}{\Omega_H^4 \dfrac{1-k^2}{\xi} - 1} \tag{12}$$

Remarkably, (10) and (11) show that $C_{\rm eq}$ differs from C_1 (and C_2) in the equivalent circuit for both resonance frequencies.[3]

Finally, since at resonance $B_1 = B_{21} = 0$, the voltage signal transmission from port 1 to port 2 is given by:

$$A_{v21,L,H} = \frac{V_2}{V_1} = \frac{G_1}{G_{21}} \tag{13}$$

where G_1 is given by (2), and G_{21} is given by (4).

In the typical case of $\xi = 1$, all the previously derived equations greatly simplify. The resonance frequencies are:

$$\omega_{L,H}^2 = \frac{\omega_0^2}{1 \pm |k|} \tag{14}$$

where $\omega_0 = \omega_1 = \omega_2$, the positive sign corresponds to the lower frequency mode, and the negative sign to the higher

[2]For $k \to 0$, B_1 is only made of the parallel combination of L_1 and C_1, such that the approximation (8) becomes inconsistent for small values of k. For $k < 0.2$, the presence of L_2 and C_2 can be practically ignored.

[3]Notice that $C_{\rm eq}$ must be larger than C_1, C_2 for the simplified model to account for the same stored energy as the transformer-based resonator. Since, at resonance, the average magnetic and electric energies are equal, the total energy stored in the resonator in Fig. 2 is $E_t = \frac{1}{2}C_1|V_1|^2 + C_2|V_2|^2 = \frac{1}{2}C_1|V_1|^2\left(1 + \frac{\xi}{n^2}\frac{|V_2|^2}{|V_1|^2}\right)$. Hence, for the circuit in Fig. 6 to show the same stored energy, $E_t = \frac{1}{2}C_{\rm eq}|V_1|^2$, $C_{\rm eq} > C_1$, C_2.

With lengthy but straightforward calculations it can be proved that the quality factor given by (7) also represents the ratio of the energy stored in the resonator, E_t, to the energy dissipated per cycle, $E_d = \frac{1}{2}G_1|V_1|^2\frac{1}{f_{\rm L,H}}$, where G_1 is given by (2) and $f_{\rm L,H} = \omega_{\rm L,H}/(2\pi)$: $Q = 2\pi E_t/E_d$. The erroneous assumption of $C_{\rm eq} = C_1$ in [10] led to the misconception that a transformer resonator would have Q defined as the energy ratio differing from Q related to the slope of the impedance phase at resonance.

frequency mode. The parameters of the simplified equivalent model are:

$$L_{\mathrm{eq,L,H}} = \frac{1 \pm |k|}{2} L_1 \qquad C_{\mathrm{eq,L,H}} = 2C_1 \tag{15}$$

and

$$R_{\mathrm{eq,L,H}} = R_{p1} \cdot \frac{(1 \pm |k|)^2}{1 + \dfrac{Q_1}{Q_2}} \tag{16}$$

where $R_{p1} = R_1 Q_1^2$ is approximately the equivalent parallel resistance of inductor L_1. The voltage signal transmission from port 1 to port 2, as given by (13), becomes:

$$A_{v21,L,H} = \pm n \tag{17}$$

The resonator quality factor, given by (7), reduces to:

$$Q \approx \frac{2Q_1Q_2}{Q_1 + Q_2}(1 \pm |k|) = \omega_{L,H} C_{\mathrm{eq,L,H}} R_{\mathrm{eq,L,H}} \tag{18}$$

To verify the accuracy of the equivalent circuit derived in this Section, Figs. 7 and 8 compare the simulated Z_{11} and Z_{21} for the networks in Figs. 2 and 6, the latter evaluated both at ω_L and ω_H. The transformer-based resonator is designed to have a lower resonance frequency at 5 GHz and $\xi = 1$. Primary and secondary coils are $L_1 = 1$ nH and $L_2 = 2$ nH, with $k = 0.75$, and $Q_1 = Q_2 = 10$ at 5 GHz. The components of the equivalent LC-tank are calculated to fit the transformer-based resonator at ω_L, and at ω_H. By using (15)–(17) we have: $L_{\mathrm{eq,L}} = 875$ pH, $L_{\mathrm{eq,H}} = 125$ pH, $C_{\mathrm{eq,L,H}} = 1.158$ pF, $R_{\mathrm{eq,L}} = 481\,\Omega$, $R_{\mathrm{eq,H}} = 69\,\Omega$, and $A_{v21,L,H} = \pm\sqrt{2}$. The simplified circuit fits very well the behavior of the transformer resonator in the neighborhood of one resonance frequency, while of course it does not capture the response at the other resonance frequency.

B. Phase Noise Analysis

Replacing the transformer-based resonator with the equivalent circuit of Fig. 6, the circuits of Fig. 1 simplify to the well-known differential-pair LC-tank oscillators. Adapting the results of [13], the phase noise at an offset angular frequency $\Delta\omega$ in the $1/f^2$ region is:

$$\mathcal{L}(\Delta\omega) = 10\log_{10}\left[\frac{N_{L,R} + N_{L,\mathrm{mos}}}{2\Delta\omega^2 C_{\mathrm{eq,L,H}}^2 V_1^2}\right] \tag{19}$$

where V_1 is the oscillation amplitude at port 1. $N_{L,R}$ and $N_{L,\mathrm{mos}}$ (simply referred to as *effective noises* hereafter) are the noise contributions from the resonator losses and the cross-coupled pair, respectively:

$$N_{L,R} + N_{L,\mathrm{mos}} = \frac{2k_BT}{R_{\mathrm{eq,L,H}}} F \tag{20}$$

where k_B is the Boltzmann's constant, and T the absolute temperature. Using the results in [15], the excess noise factor, F, is written as:

$$F = \begin{cases} 1 + \gamma & \text{one-port oscillator} \\ 1 + \dfrac{\gamma}{A_{v21,L,H}} & \text{two-port oscillator} \end{cases} \tag{21}$$

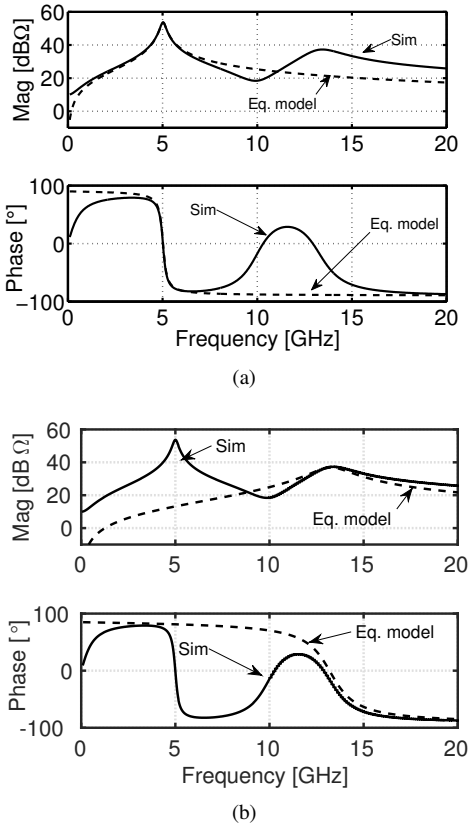

Fig. 7. Simulated Z_{11} (magnitude and phase) for the transformer-based resonator in Fig. 2 and the equivalent circuit in Fig. 6 evaluated at: (a) ω_L, (b) ω_H.

F captures the difference between the two oscillators in Fig. 1, i.e. the effective noise generated by the transistors in the two-port oscillators is divided by the voltage transfer, $A_{v21,L,H}$, between the two ports of the resonator.

Expressing the resonator quality factor as $Q(\omega_{L,H}) = \omega_{L,H} C_{\mathrm{eq,L,H}} R_{\mathrm{eq,L,H}}$, and replacing (20) and (21) in (19), the phase noise of the two oscillators is written as:

$$\mathcal{L}(\Delta\omega) = 10\log_{10}\left[\frac{k_BTFR_{\mathrm{eq,L,H}}}{V_1^2} \cdot \left(\frac{\omega_{L,H}}{Q(\omega_{L,H})\Delta\omega}\right)^2\right] \tag{22}$$

Equation (22) is valid for arbitrary values of the resonator parameters, and for oscillators leveraging either of the two resonance frequencies, $\omega_{L,H}$.

To gain further insight, (22) can be elaborated by considering a typical design scenario where: first, the transformer windings have the same quality factor, $Q_1 = Q_2 = Q_{1,2}$, and, second, $\xi = 1$ to maximize the resonator Q. With these assumptions, by using (16) and (18), and expressing V_1 in (22) as a function of the bias current I_b and $R_{\mathrm{eq,L,H}}$, the phase noise can be recast as a function of I_b, $\omega_{L,H}$, and the parameters of the transformer-based resonator. In class-B differential LC oscillators, the tank current resembles a square wave with a fundamental component of $(2/\pi)I_b$ and the oscillation amplitude, in the current limited regime, is

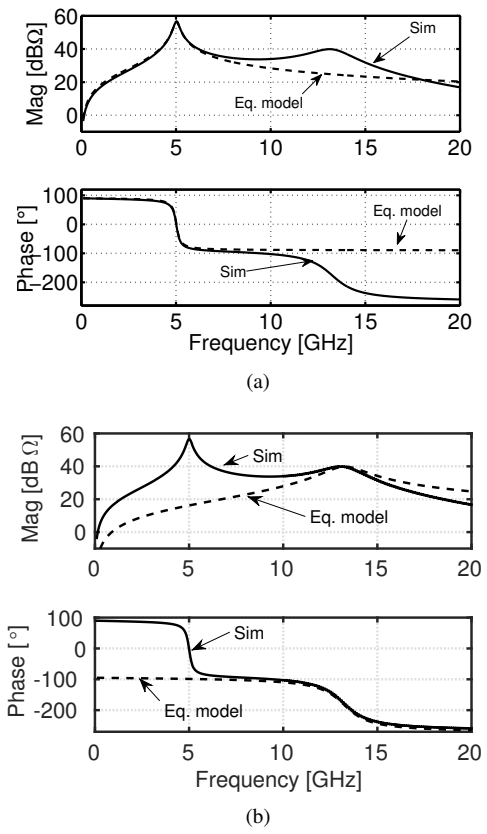

Fig. 8. Simulated Z_{21} (magnitude and phase) for the transformer-based resonator in Fig. 2 and the equivalent circuit in Fig. 6 evaluated at: (a) ω_L, (b) ω_H.

$V_1 = (2/\pi)R_{\mathrm{eq,L,H}}I_b$. The phase noise is hence written as:

$$\mathcal{L}(\Delta\omega) = 10\log_{10}\left[\frac{k_BTF}{2(I_b/\pi)^2R_{p1}(1\pm|k|)^4}\left(\frac{\omega_{L,H}}{Q_{1,2}\Delta\omega}\right)^2\right] \quad (23)$$

This equation highlights a strong dependency of the phase noise on the magnetic coupling coefficient between the transformer inductors, k. Note that (23) is substantially valid for class-C differential LC oscillators as well, the only difference being that, in class-C operation, the amplitude of the fundamental component of the tank current is $\approx I_b$ as opposed to $(2/\pi)I_b$, i.e. class-C biasing features a higher current conversion efficiency.

IV. Simulation Results

To gain insight and also prove the accuracy of the analysis, SpectreRF phase noise simulations at 1 MHz offset from the carrier versus the magnetic coupling coefficient k are shown in Fig. 9, and compared with (23) for oscillators tuned at ω_H and ω_L, respectively.

The resonator has been designed with the following parameters: 5 GHz oscillation frequency, $Q_{1,2} = 10$, $L_1 = 1$ nH, $L_2 = 2$ nH, yielding $A_{v21,L,H} = \pm\sqrt{2}$, and $\xi = 1$. The excess noise factor is given by (21), in which $\gamma = 2/3$ is set.

First, the resonator is operated leveraging the mode at ω_H. For $\xi = 1$, only the two-port oscillator topology of Fig. 1(b) is capable of starting up the oscillations at the higher-frequency mode [1]. Hence, the simulation results in Fig. 9(a) are reported for this topology only. The plot compares the calculated and simulated phase noise at 1 MHz offset from the carrier when k is raised from 0.2 to 0.8. When the resonator is operated at ω_H the impedance decreases rapidly when k is raised (as expected from (16)). To satisfy the start-up condition up to the highest considered value of k, the bias current is set to 25 mA and a very large transistor aspect ratio is used (550 μm / 0.25 μm). The simulated voltage swing at port 1 decreases from $V_1 = 2.6$ V, attained for $k = 0.2$, down to $V_1 = 0.2$ V, with $k = 0.7$. Fig. 9(a) proves a very good agreement between the calculated and simulated phase noise. As predicted by (23), the phase noise rises (by some 20 dB) as k is increased from 0.2 to 0.7. This is because, when the transformer resonator is used at ω_H, a higher magnetic coupling results in both a lower quality factor and lower equivalent resistance, impairing both the phase noise performance and the oscillator Figure-of-Merit.

Next, the resonator is operated leveraging the mode at ω_L. In this case, the bias current and transistors size are reduced to 5 mA and 70 μm / 0.25 μm, respectively, and both the one-port and two-port circuit configurations are considered. Figure 1(b) compares the simulated and calculated phase noise at 1 MHz offset, still demonstrating very good agreement. The plot shows an improvement in phase noise of ≈ 10 dB when k is raised from 0.2 to 1. A similar agreement between simulations and theory is found over a broad range of design parameters. When the resonator is operated at ω_L, the increase in the mutual magnetic inductance between the coupled coils leads to both a higher resonator Q and a larger equivalent resistance at resonance, $R_{\mathrm{eq,L}}$. The latter improves the phase noise as long as it results in an increase of the oscillation amplitude i.e. as long as the oscillator works in the current limited region. In the simulations of Fig. 9(b), the voltage swing at port 1 ranges from $V_1 = 730$ mV, with $k = 0.2$, to $V_1 = 2$ V, with $k = 1$.

As with the LC-tank oscillators, (22) shows that for a given technology and resonator, i.e. $R_{\mathrm{eq,L,H}}$ and Q, the ultimately lower phase noise level is achieved when the bias current is set to maximize V_1=$V_{1,\max}$, bounded by the supply voltage. If a lower phase noise is required, the equivalent resistance at resonance, $R_{\mathrm{eq,L,H}}$, can be scaled down, while increasing the bias current (i.e. the power dissipation) to restore $V_{1,\max}$.

To further validate the proposed phase noise analysis, a planar transformer with a 2:1 turn ratio has been laid out in a 6-layer CMOS metal stack. The geometry is shown in Fig. 10(a). The two interleaved windings, realized by shorting together the two topmost metal layers, are 10 μm spaced and 12 μm wide. The internal diameter is 330 μm.

S-parameters have been derived from Electromagnetic (EM) simulations with the purpose of estimating the component performance and building an equivalent circuit model used for oscillator phase noise simulations. The lumped-element equivalent circuit is reported in Fig. 10(b); the corresponding component values are reported in Table I. Metal trace and substrate losses are accounted for by resistors $R_{s1,2}$ and $R_{\mathrm{sub1,2}}$, respectively.

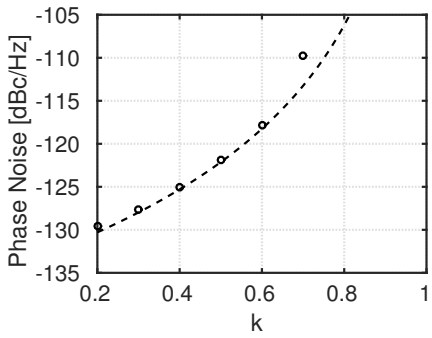

(a)

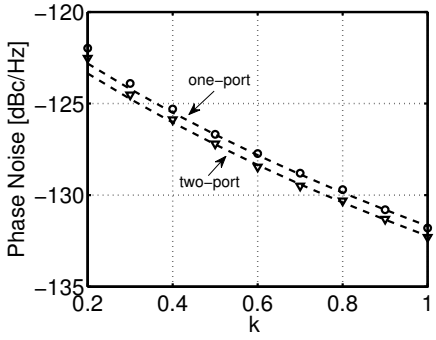

(b)

Fig. 9. Simulated (dots) and calculated (lines) phase noise at 1 MHz offset from the carrier for the one-port and two-port oscillators operated in: (a) higher frequency mode, ω_H, (b) lower frequency mode, ω_L. In all cases, the oscillators are operated at 5 GHz.

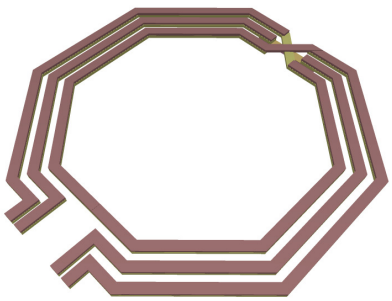

(a)

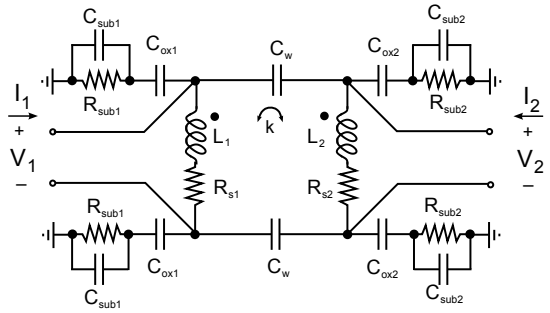

(b)

Fig. 10. A 2:1 planar transformer in a 6-metal CMOS technology: (a) layout, (b) equivalent circuit model.

TABLE I
COMPONENT VALUES OF THE TRANSFORMER EQUIVALENT CIRCUIT MODEL IN FIG. 10

L_1	R_{s1}	$C_{\rm ox1}$	$C_{\rm sub1}$	$R_{\rm sub1}$	k
1 nH	2.5 Ω	70 fF	16 fF	4 kΩ	0.65

L_2	R_{s2}	$C_{\rm ox2}$	$C_{\rm sub2}$	$R_{\rm sub2}$	C_w
2.74 nH	4.6 Ω	189 fF	43 fF	1.5 kΩ	10 fF

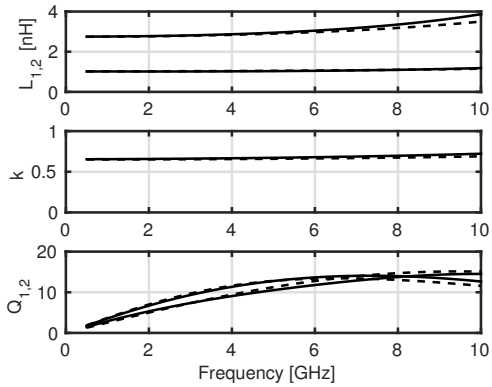

Fig. 11. Inductances, k, and windings quality factors from EM simulations (solid line) and from the transformer circuit model in Fig. 10(b) (dashed line).

Figure 11 compares the transformer inductances, k and quality factors derived from EM simulations with results from the equivalent circuit model. Despite the simplicity of the model, good fit is achieved over a wide frequency range. The two ports of the transformer are tuned with capacitors to achieve 5 GHz lower resonance frequency with $\xi = 1$. From the simulations reported in Fig. 11, the primary and secondary quality factors are $Q_1 \approx 10.6$ and $Q_2 \approx 12.8$, respectively, and $k = 0.65$. Equation (18) predicts a Q for the tuned transformer of 19.1 while the simulated value is 17.5. The small discrepancy can be attributed to substrate losses, not considered in the analysis leading to (18), that limit the improvement achievable by means of magnetic coupling between the coils. Substrate losses are also responsible of a slight overestimation of the equivalent resistance at resonance of port 1: simulations show $R_{\rm eq,L} = 445\,\Omega$, while (16) yields $R_{\rm eq,L} = 504\,\Omega$.

The double tuned transformer has been used as a resonator for the one- and two-port oscillator topologies of Fig. 1. With a 5 mA bias current, the simulated oscillation amplitude at port 1 is $V_1 = 1.41$ V and the phase noise at 1 MHz offset from the 5 GHz carrier is -128.8 dBc/Hz and -129.8 dBc/Hz, for the one- and two-port topologies, respectively. The corresponding values predicted by (22) using the calculated Q are -129.8 dBc/Hz and -130.5 dBc/Hz, slightly optimistic because of the overestimation of Q due to (16). Indeed, if the calculated value of Q is replaced with the simulated one, (22) estimates a phase noise for the one- and two-port oscillators of -129 dBc/Hz and -129.8 dBc/Hz, respectively, in excellent agreement with SpectreRF simulations.

V. Discussion and Conclusion

The presented analysis shows that the phase noise performance of double-tuned transformer oscillators is only determined by the resonator characteristics near the oscillation frequency. The multi-resonance transfer function of double-tuned transformers does not provide any intrinsic benefit because phase noise is only determined by the quality factor and impedance at the oscillation frequency, exactly as in the case of simple LC-tank oscillators. Magnetic coupling between the transformer windings improves the resonator quality factor. On the other hand, the same magnetic coupling is still present even if the transformer windings are arranged to form a single multi-turn spiral, as previously pointed out in [11], [12]. To gain further insights, we compare the performance of an oscillator built around a transformer-based resonator with respect to the use of the two simple LC-tanks shown in Fig. 12, where the inductor is realized by connecting in series or in parallel the two coupled coils of a transformer. As detailed in the Appendix, the condition that maximizes the tank quality factor is $Q_1 = Q_2$, and they are both equal to their maximum achievable value, similarly to the case of the transformer-based resonator. Furthermore, if $Q_1 = Q_2$, the value of n that maximizes Q is $n = 1$. As a consequence, in the following discussion we assume $L_1 = L_2$ and $R_1 = R_2$.

First, let us consider the tank in Fig. 12 (a). As shown in the Appendix, the quality factor is $Q = Q_{1,2}(1 + |k|)$, the same displayed at ω_L by the transformer resonator with $\xi = 1$. On the other hand, the equivalent resistances at resonance are remarkably different. By inspection of the circuit in Fig. 12(a), $R_{\mathrm{eq,tank}} = 2R_{p1}(1 + |k|)^2$. From (16), the transformer resonator has a fourfold lower resistance: $R_{\mathrm{eq,L}} = 0.5R_{p1}(1+|k|)^2$. As a consequence, the transformer resonator can be exploited to target a lower phase noise because, as per (22), the minimum achievable phase noise will as well be fourfold lower. This phase noise improvement, of course, does not come for free. In fact the bias current (and hence power dissipation) needed to obtain $V_{1,\max}$ is four times higher. As a result, the oscillator Figure-of-Merit, normalizing phase noise to power dissipation, is not improved by the use of the transformer resonator.

We consider now the LC-tank in Fig. 12(b), where the inductor is realized by shunting the two transformer coils. The quality factor is still $Q = Q_{1,2}(1+|k|)$ (see Appendix), while the tank resistance at resonance is $R_{\mathrm{eq,tank}} = 0.5R_{p1}(1+|k|)^2$, the same given by (16) for the transformer resonator. Thus, if the simple LC-tank in Fig. 12(b) replaces the transformer-based resonator in the oscillator of Fig. 1(a), the same phase noise is attained, while dissipating the same amount of power. As a result, even in this case the transformer-based resonator does not provide any fundamental advantage both in terms of Figure-of-Merit and minimum achievable phase noise.

We compared, by means of SpectreRF simulations, the one-port transformer-based oscillator in Fig. 1(a) against two LC-tank oscillators with the resonators in Fig. 12(a) and (b). The following design parameters were considered: 5 GHz oscillation frequency, $L_1 = L_2 = 1\,\mathrm{nH}$, $k = 0.75$, $Q_1 = Q_2 = 10$. The bias current (I_b) was set to achieve the same

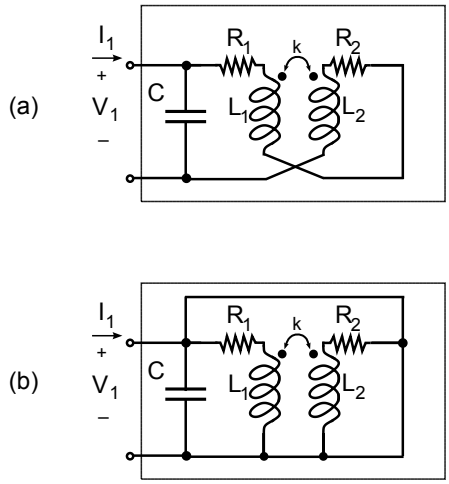

Fig. 12. LC-tank using two coupled coils connected in: (a) series, (b) parallel.

oscillation amplitude (V_1) in all cases. For the oscillator with transformer-based resonator we have: $I_b = 5\,\mathrm{mA}$, $V_1 = 1.53\,\mathrm{V}$, $\mathcal{L}(1\,\mathrm{MHz}) = -129.3\,\mathrm{dBc/Hz}$. For the oscillator with the LC-tank in Fig. 12(a) we get: $I_b = 1.25\,\mathrm{mA}$, $V_1 = 1.527\,\mathrm{V}$, $\mathcal{L}(1\,\mathrm{MHz}) = -123.5\,\mathrm{dBc/Hz}$. Eventually, for the oscillator with the LC-tank in Fig. 12(b) we obtain: $I_b = 5\,\mathrm{mA}$, $V_1 = 1.53\,\mathrm{V}$, $\mathcal{L}(1\,\mathrm{MHz}) = -129.4\,\mathrm{dBc/Hz}$. The LC-tank in Fig. 12(a) (achieved by connecting in series the two transformer coils) shows the same Q of the transformer-based resonator but four times the resistance at resonance. Therefore, the oscillator needs 4 times lower bias current to achieve the same voltage swing but yields a 6 dB higher phase noise. The oscillator with the LC-tank in Fig. 12(b) (achieved by connecting in parallel the two transformer coils) yields exactly the same performance of the transformer-based oscillator: same voltage swing and same phase noise for the same bias current.

Finally, it is worth to consider the merits of the two-port configuration. As shown in (21), and confirmed in Fig. 9, this topology allows reducing the effective noise generated by the active devices if $A_{v21,L,H} > 1$. However, it must be emphasized that the decrease in the phase noise is due to the voltage gain provided by the transformer, and not to the higher order of the resonator. Moreover, if the oscillator is biased to achieve $V_{1,\max}$, reliability concerns might prevent to set $V_2 \gg V_{1,\max}$, such that the decrease of $N_{L,\mathrm{mos}}$ is very limited. The issue can be partially mitigated by using thick-oxide devices.

Another remarkable advantage of the two-port configuration is the dc decoupling between the gate and drain nodes of the active devices, that allows to optimize the bias point and large-signal operation of the transistors [15], [19], [20]. Moreover, a two-port oscillator with transformer-based resonator has been recently proposed to limit $1/f$ noise upconversion into phase noise [21].

In conclusion, the rigorous, yet simple, equivalent model proposed in this paper discloses a manageable analysis of harmonic oscillators with transformer-based resonators. The latter, while being amenable to wide tuning range operation,

or optimization of the transistors quiescent point and voltage swings, do not show any fundamental advantage in terms of minimum achievable $1/f^2$ phase noise or Figure-of-Merit, as compared to oscillators with conventional LC-tanks, because of the intrinsic features of a high-order resonator.

APPENDIX

Connecting the two coupled coils in series as in Fig. 12(a) turns the transformer in a one-port device, whose impedance is:

$$Z_1 = R_1 + R_2 + j\omega(L_1 + L_2)(1 + \frac{2nk}{1+n^2}) \qquad (24)$$

The quality factor is:

$$Q = Q_1 \frac{1 + 2nk + n^2}{1 + n^2 \frac{Q_1}{Q_2}}. \qquad (25)$$

Notice that (25), likewise (7), can be recast in the form

$$Q = A \frac{Q_1 Q_2}{Q_1 + B\, Q_2}, \qquad (26)$$

where $A, B \geq 0$, proving that Q is an increasing monotonic function of Q_1 and Q_2. Hence, any effort to increase Q_1 or Q_2 will result in an increase of Q. The maximum Q is clearly obtained when $Q_1 = Q_2$, and they are both equal to their maximum achievable value. If $Q_1/Q_2 = 1$, (25) shows that the quality factor is maximized, for any value of k, if $n = 1$.

If the two coupled coils of the transformer are connected in parallel as in Fig. 12(b), the impedance of the resulting one-port device can be approximated as:

$$Z_1 \approx \frac{R_1 R_2}{R_1 + R_2} + j\omega \frac{L_1 L_2}{L_1 + L_2} \frac{1 - k^2}{1 - \frac{2nk}{1+n^2}} \qquad (27)$$

Hence, the quality factor is:

$$Q = \frac{Q_2 + Q_1 n^2}{1 + n^2} \frac{1 - k^2}{1 - \frac{2nk}{1+n^2}} \qquad (28)$$

Clearly, (28) shows that Q is an increasing monotonic function of Q_1 and Q_2. Likewise the case of the transformer-based resonator, and of the series connected coupled coils, the condition that maximizes Q is $Q_1 = Q_2$, and they are both equal to their maximum achievable value. If $Q_1/Q_2 = 1$, (28) shows that the value of n that maximizes Q, for any value of k, is $n = 1$.

REFERENCES

[1] A. Bevilacqua, F. P. Pavan, C. Sandner, A. Gerosa, and A. Neviani, "Transformer-based dual-mode voltage controlled oscillators," *IEEE Trans. on Circuits and Systems II: Express Briefs*, vol. 54, no. 4, pp. 293–297, 2007.

[2] B. Catli and M. Hella, "A 1.94 to 2.55 GHz, 3.6 to 4.77 GHz tunable CMOS VCO based on double-tuned, double-driven coupled resonators," *IEEE Journal of Solid-State Circuits*, vol. 44, no. 9, pp. 2463–2477, 2009.

[3] Z. Safarian and H. Hashemi, "Wideband multi-mode CMOS VCO design using coupled inductors," *IEEE Transactions on Circuits and Systems I: Regular Papers*, vol. 56, no. 8, pp. 1830–1843, 2009.

[4] G. Li, L. Liu, Y. Tang, and E. Afshari, "A low-phase-noise wide-tuning-range oscillator based on resonant mode switching," *IEEE Journal of Solid-State Circuits*, vol. 47, no. 6, pp. 1295–1308, June 2012.

[5] S. Rong and H. Luong, "Analysis and design of transformer-based dual-band VCO for software-defined radios," *IEEE Transactions on Circuits and Systems I: Regular Papers*, vol. 59, no. 3, pp. 449–462, March 2012.

[6] J. Borremans, A. Bevilacqua, S. Bronckers, M. Dehan, M. Kuijk, P. Wambacq, and J. Craninckx, "A compact wideband front-end using a single-inductor dual-band vco in 90 nm digital cmos," *Solid-State Circuits, IEEE Journal of*, vol. 43, no. 12, pp. 2693–2705, Dec 2008.

[7] M. Straayer, J. Cabanillas, and G. M. Rebeiz, "A low-noise transformer-based 1.7GHz CMOS VCO," in *IEEE ISSCC Digest of Technical Papers*, San Francisco, CA, Feb 2002, pp. 286–287.

[8] D. Baek, T. Song, S. Ko, E. Yoon, and S. Hong, "Analysis on resonator coupling and its application to CMOS quadrature VCO at 8 GHz," in *IEEE Radio Frequency Integrated Circuits (RFIC) Symposium*, 2003, pp. 85–88.

[9] A. El-Gouhary and N. Neihart, "Analysis of transformer-based resonator quality factor and bandwidth and the implications to VCOs," in *2011 IEEE International Symposium on Circuits and Systems (ISCAS)*, May 2011, pp. 1888–1891.

[10] ——, "An analysis of phase noise in transformer-based dual-tank oscillators," *IEEE Transactions on Circuits and Systems I: Regular Papers*, vol. 61, no. 7, pp. 2098–2109, July 2014.

[11] H. Krishnaswamy and H. Hashemi, "Inductor- and transformer-based integrated RF oscillators: A comparative study," in *IEEE Custom Integrated Circuits Conference*, 2006, pp. 381–384.

[12] P. Andreani and J. Long, "Misconception regarding use of transformer resonators in monolithic oscillators," *Electronics Letters*, vol. 42, no. 7, pp. 387–388, 2006.

[13] P. Andreani, X. Wang, L. Vandi, and A. Fard, "A study of phase noise in Colpitts and LC-tank CMOS oscillators," *IEEE Journal of Solid-State Circuits*, vol. 40, no. 5, pp. 1107–1118, 2005.

[14] P. Andreani and A. Fard, "An analysis of $1/f^2$ phase noise in bipolar Colpitts oscillators (with a digression on bipolar differential-pair LC oscillators)," *IEEE Journal of Solid-State Circuits*, vol. 42, no. 2, pp. 374–384, 2007.

[15] A. Mazzanti and P. Andreani, "Class-C harmonic CMOS VCOs, with a general result on phase noise," *IEEE Journal of Solid-State Circuits*, vol. 43, no. 12, pp. 2716–2729, 2008.

[16] ——, "A push–pull class-C CMOS VCO," *IEEE Journal of Solid-State Circuits*, vol. 48, no. 3, pp. 724–732, March 2013.

[17] A. Bevilacqua and P. Andreani, "Phase noise analysis of the tuned-input–tuned-output (TITO) oscillator," *IEEE Transactions on Circuits and Systems II: Express Briefs*, vol. 59, no. 1, pp. 20–24, Jan 2012.

[18] O. Takashi, "Rigorous Q-factor formulation for one- and two-port passive linear networks from an oscillator noise spectrum viewpoint," *IEEE Transactions on Circuits and Systems-II: Express Briefs*, vol. 52, no. 12, pp. 846–850, 2005.

[19] A. Visweswaran, R. Staszewski, and J. Long, "A clip-and-restore technique for phase desensitization in a 1.2V 65nm CMOS oscillator for cellular mobile and base stations," in *2012 IEEE International Solid-State Circuits Conference Digest of Technical Papers (ISSCC)*, Feb 2012, pp. 350–352.

[20] M. Babaie and R. Staszewski, "Third-harmonic injection technique applied to a 5.87-to-7.56GHz 65nm CMOS Class-F oscillator with 192dbc/hz FOM," in *2013 IEEE International Solid-State Circuits Conference Digest of Technical Papers,*, Feb 2013, pp. 348–349.

[21] M. Shahmohammadi, M. Babaie, and R. Staszewski, "A 1/f noise upconversion reduction technique applied to Class-D and Class-F oscillators," in *2015 IEEE International Solid- State Circuits Conference,*, Feb 2015, pp. 1–3.

Andrea Mazzanti received the Laurea and Ph.D. degrees in electrical engineering from the Università di Modena and Reggio Emilia, Modena, Italy, in 2001 and 2005, respectively. During the summer of 2003, he was with Agere Systems, Allentown, PA as an Intern. From 2006 to 2009, he was Assistant Professor with the Università di Modena and Reggio Emilia. In January 2010, he joined the Università di Pavia where he is now Associate Professor. He has authored over 80 technical papers. His main research interests cover device modeling and IC design for high-speed communications, RF and millimeter-wave systems. Dr. Mazzanti has been a member of the Technical Program Committee of the IEEE Custom Integrated Circuit Conference (CICC) from 2008 to 2014, IEEE European Solid State Circuits Conference (ESSCIRC) and IEEE International solid State Circuits Conference (ISSCC) since 2014. He was Guest Editor for the special issue of the Journal of Solid State Circuits dedicated to CICC-2013 and he is currently Associate Editor for the Transactions on Circuits and Systems-I.

Andrea Bevilacqua (S'02, M'04, SM'14) received the Laurea, and Ph.D. degrees in electronics engineering from the University of Padova, Padova, Italy, in 2000, and 2004, respectively. From 2005 to 2015 he was an Assistant Professor with the Department of Information Engineering, University of Padova, where he is now an Associate Professor. His current research interests include the design of RF/microwave integrated circuits and the analysis of wireless communication and radar systems. He is author or coauthor of more than 60 technical papers, and he holds 2 patents. Dr. Bevilacqua has been serving as a member of the TPC of IEEE ESSCIRC since 2007, and was TPC Co-Chair of IEEE ESSCIRC 2014. He was a member of the TPC of IEEE ICUWB from 2008 to 2010. He was an Associate Editor of IEEE TCAS-II from 2011 to 2013 and was nominated Best Associate Editor for TCAS-II for 2012 to 2013.